


Band Structure, Charge Distribution and Optical Properties of $\text{AlP}_x\text{Sb}_{1-x}$ Ternary Semiconductor Alloys

Nour-El-Houda Fares^a, Nadir Bouarissa^{b*} 

^aUniversity of Bordj Bou Arreridj, Laboratory of Materials and Electronic Systems, 34000, Bordj Bou Arreridj, Algeria

^bUniversity of M'sila, Laboratory of Materials Physics and its Applications, 28000, M'sila, Algeria

Received: October 27, 2017; Revised: February 09, 2018; Accepted: March 19, 2018

The present contribution studies on the composition dependence of the electronic and optical properties of the zinc-blende alloy system $\text{AlP}_x\text{Sb}_{1-x}$. The calculations are performed using a pseudopotential approach under the virtual crystal approximation. Features such as electronic band structure, energy band-gaps, refractive index, dielectric constants and valence and conduction charge densities are determined and their compositional dependence are examined and discussed. The aim of this paper is to provide new data for electronic and optical properties by varying the alloy composition x and to see to what extent the compositional disorder affects the properties of interest. The effect of alloy disorder on the energy band-gaps and electron charge densities is found to be important for getting a meaningful agreement with experiment. Our results show a direct-band gap bowing parameter of 2.7 eV which agrees very well with experiment. Moreover, a transition between indirect band gaps is found to occur twice. Besides, bonding and ionicity are discussed in terms of electron charge distribution. The information derived from the present study can be useful for optoelectronics applications.

Keywords: *Electronic structure, charge densities, optical properties, $\text{AlP}_x\text{Sb}_{1-x}$ alloys, optoelectronics.*

1. Introduction

The electronic band structure and optical properties of III-V and II-VI zinc-blende semiconductors have been widely described experimentally and theoretically for many years¹⁻⁶. Generally, special attention is paid to the structure of the band around the maximum of the valence band and the minimum of the conduction band, because these features are of particular interest for the transport properties. AlSb is a semiconductor of group III-V family which has an indirect band-gap (Γ -X). Recently, this material has found considerable use as the barrier in long-wavelength optoelectronic devices⁷ as well as in high-mobility electronic devices^{1,8}. On the other hand, AlP is also a III-V semiconductor with an indirect band-gap. This material can be alloyed with other binary compound semiconductors. This may be useful in devices such as light-emitting diodes. In recent years, the successful growth of $\text{AlP}_{0.40}\text{Sb}_{0.60}$ lattice matched to InP has been reported⁹. This has encouraged people to investigate the properties of $\text{AlP}_x\text{Sb}_{1-x}$ ternary semiconductor alloys^{1,10}.

In the current contribution, the electronic band structure, electron valence and conduction charge densities and optical properties of $\text{AlP}_x\text{Sb}_{1-x}$ have been studied. The aim of this work is to obtain new electronic and optical properties that

were not possible in the parent compound semiconductors AlSb and AlP by varying the alloy composition x . The calculations are performed using essentially the empirical pseudopotential method (EPM) within the virtual crystal approximation (VCA) that takes into consideration the compositional disorder effect.

2. Computational Details

The EPM has been mainly used for the present calculations. It is an approach which involves a direct fit of the atomic form factors to experiment¹¹. The method was applied to several semiconductors with surprisingly good results¹¹⁻¹⁴. The crystal potential $V(\mathbf{r})$ is represented by a linear superposition of atomic potentials. For an electron in the crystal, the pseudopotential Hamiltonian is written as,

$$H = \frac{-\hbar^2}{2m^*} \nabla^2 + V(\mathbf{r}) \quad (1)$$

The solution of the equation,

$$\left[\frac{P^2}{2m} + V(\mathbf{r}) \right] \psi_{n,k}(\mathbf{r}) = E_n(k) \psi_{n,k}(\mathbf{r}) \quad (2)$$

*e-mail: n_bouarissa@yahoo.fr

gives the pseudo wave functions $\psi_{n,k}(r)$ and the band energy values $E_n(k)$, where n is the band index. The $\psi_{n,k}(r)$ have the Bloch form. These pseudo wave functions have been expanded in a set of plane waves. By solving the relevant secular equation, the expansion coefficients can be determined.

A set of symmetrical and anti-symmetrical pseudopotential form factors has been adjusted so as to get direct and indirect band-gap energies that are in accord with experiment. The optimization of the empirical pseudopotential parameters has been made using the non-linear least-squares method. More details about the method used can be found in Refs.¹⁵⁻¹⁷. The experimental band-gap energies at Γ , X and L high-symmetry points in the Brillouin zone used in the fitting procedure for AlSb and AlP are given in Table 1. The final symmetric V_s and antisymmetric V_A pseudopotential form factors obtained in the present paper from adjustments and the used lattice constants for AlSb and AlP are listed in Table 2.

The potential of $\text{AlP}_x\text{Sb}_{1-x}$ ternary semiconductor alloys is determined using the VCA which includes the compositional disorder effect as an effective potential. More details about the used approximation can be found in Refs.¹⁹⁻²¹. The Vegard's law²² has been used so as to obtain the lattice constant of the material under investigation.

The electron charge density is computed using wave functions determined from the electron band structure calculations, where the total charge distribution is expressed as,

$$\rho(r) = \sum_n \sum_k e |\psi_{n,k}(r)|^2 \quad (3)$$

In Eq.(3), $\psi_{n,k}(r)$ are the electron wave functions whereas n is the band index.

The summations are generally taken over all states in the Brillouin zone for all occupied bands. Nevertheless, in this work we are only interested in charge density at the Γ point in the Brillouin zone. Hence, Eq. (3) can be written as,

$$\rho(r) = e |\psi_{n,k}(r)|^2 \quad (4)$$

Table 1. Experimental bandgap energies for AlSb and AlP fixed in the fits.

Compound	$E_{\Gamma-\Gamma}$ (eV)	$E_{\Gamma-X}$ (eV)	$E_{\Gamma-L}$ (eV)
AlSb	2.30 ¹⁸	1.615 ¹⁸	2.211 ¹⁸
AlP	3.56 ¹	2.52 ¹	3.57 ¹

Table 2. Pseudopotential parameters for AlSb and AlP.

Compound	Form factors (Ry)						Lattice constant (\AA)
	$V_s(3)$	$V_s(8)$	$V_s(11)$	$V_A(3)$	$V_A(4)$	$V_A(11)$	
AlSb	-0.225597	0.028086	0.062230	0.007109	0.058960	0.004544	6.1355
AlP	-0.241305	0.021262	0.249336	0.030061	0.116000	0.232543	5.4635

3. Results and Discussion

Figures 1a-1c display the computed electron energy band structures along selected symmetry directions in the Brillouin zone for zinc-blende AlSb, $\text{AlP}_{0.05}\text{Sb}_{0.95}$ and $\text{AlP}_{0.1}\text{Sb}_{0.9}$, respectively. The maximum of the valence band is assumed to be the zero energy for all band structures of interest. All band structures look rather similar. The main difference appears to be in their fundamental energy band-gap. In fact, in Fig.1a one can note that the maximum of the valence band is at Γ point, whereas the minimum of the conduction band is at X point. Hence, AlSb is an indirect-gap (Γ -X) semiconductor. The same conclusion can be drawn for $\text{AlP}_{0.05}\text{Sb}_{0.95}$ (Fig.1b). However, as far as $\text{AlP}_{0.1}\text{Sb}_{0.9}$ is concerned and as can be seen in Fig.1c, the maximum of the valence band is at Γ point, whereas the minimum of the conduction band is at L point. Thus, $\text{AlP}_{0.1}\text{Sb}_{0.9}$ is an indirect-gap (Γ -L) semiconductor. These results for Figs. 1b and 1c are obtained when the compositional disorder effect is taken into consideration. The disorder effect as can be noticed from these figures has an important effect on the electronic band structure and should not be neglected. The full valence band width seems to increase with increasing the P content (even at low concentrations of P). This reflects the change in the ionicity of AlSb when more P atoms are added in it.

In order to see to what extent the alloy compositional disorder effect can affect the band-gap energies, the composition dependence of band-gap for conduction Γ and X valleys with respect to the top of the valence band in $\text{AlP}_x\text{Sb}_{1-x}$ is displayed in Figs.2a and 2b, respectively. For both figures the calculations have been performed using the VCA (where the compositional disorder is neglected) and the improved VCA (where the compositional disorder is taken into account in the calculations). By observing Fig.2a, one can note that when proceeding from AlSb ($x=0$) to AlP ($x=1$) the direct (Γ - Γ) band gap increases in both cases (with and without considering the compositional disorder effect). The two approaches exhibit the same behavior, which is non monotonic. However, the non linearity seems to be different. Accordingly, one of course expects different optical band gap bowing parameters. In fact, when using the VCA alone, we found an optical band-gap bowing parameter of -2.07 eV. This value is not in accord with that of 2.7 eV recommended by Vurgaftman et al.¹, both in sign and magnitude. Nevertheless, the use of the improved VCA yields an optical bowing parameter for the Γ -valley of 2.7 eV. This result is obtained for the disorder

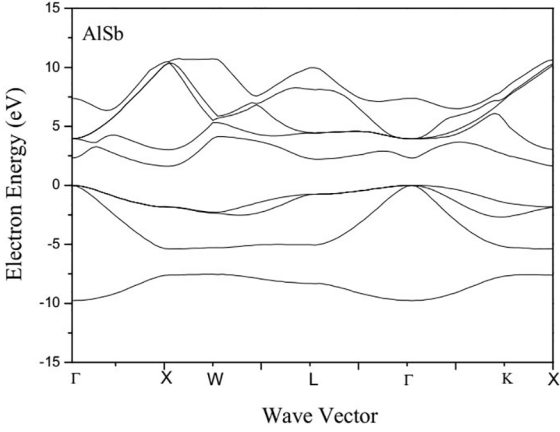


Figure 1 a.

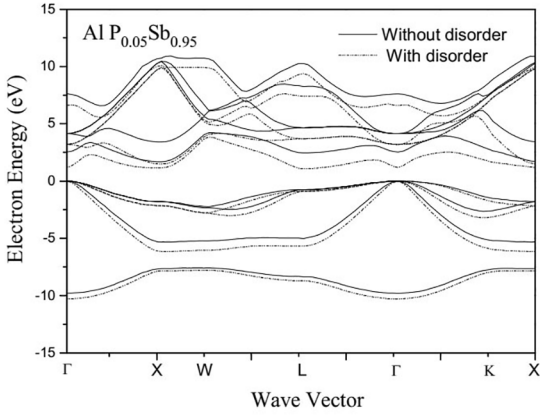


Figure 1 b.

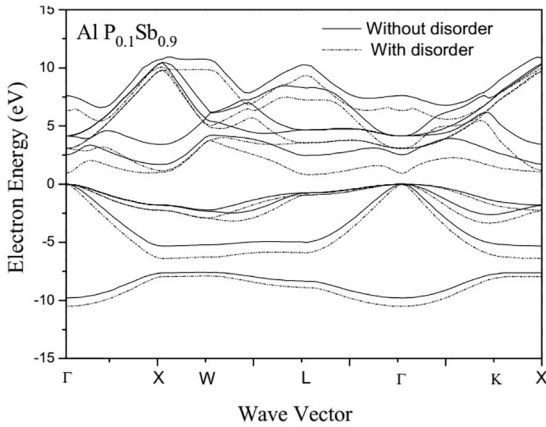


Figure 1 c.

Figure 1. (a) Electron band structure for AlSb. (b) Electron band structure for $\text{AlP}_{0.05}\text{Sb}_{0.95}$. (c) Electron band structure for $\text{AlP}_{0.1}\text{Sb}_{0.9}$.

parameter $P=0.973$ and is in excellent agreement with that recommended by Vurgaftman et al.¹, reflecting thus the important contribution of the compositional disorder to the determination of the direct (Γ - Γ) band-gap optical bowing parameter in $\text{AlP}_x\text{Sb}_{1-x}$ ternary alloys. This seems to be common for most of III-V and II-VI ternary semiconductor alloys^{23,24}. The situation seems to be somewhat different for the indirect band gap energy (Γ -X) in $\text{AlP}_x\text{Sb}_{1-x}$ (see Fig.2b). We note that the (Γ -X) energy band-gap varies monotonically with the alloy composition x with a bowing parameter of -0.64 eV when using the VCA alone. However, we observe a non-monotonic behavior of (Γ -X) band-gap versus x with a huge bowing parameter of 4.2 eV when the improved VCA has been used. Once again this demonstrates the important contribution of the compositional disorder effect to the band-gaps bowing parameters.

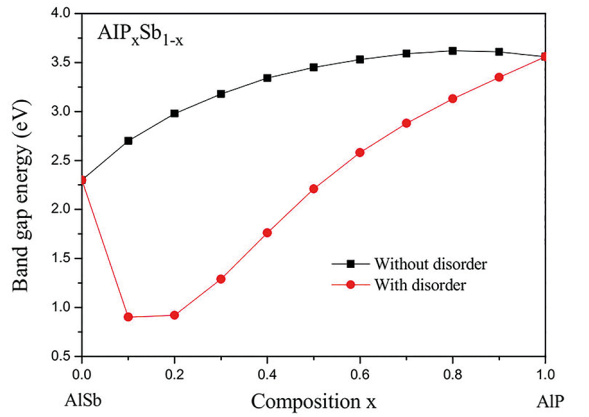


Fig. 2(a)

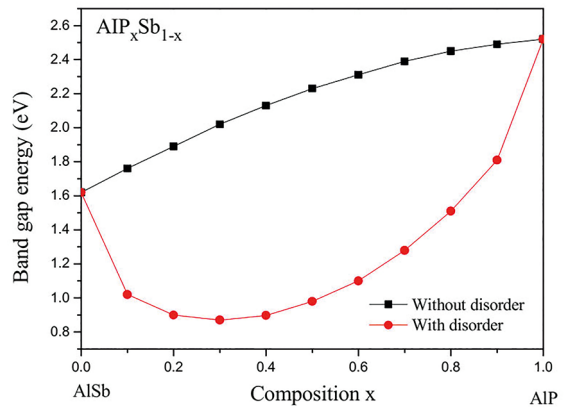


Fig. 2(b)

Figure 2. (a) Direct (Γ - Γ) band gap energy in $\text{AlP}_x\text{Sb}_{1-x}$ ternary alloys versus P content calculated with and without considering the compositional disorder effect. (b) Indirect (Γ -X) band gap energy in $\text{AlP}_x\text{Sb}_{1-x}$ ternary alloys versus P content calculated with and without considering the compositional disorder effect.

To examine the energy band-gaps transition, the three major valleys at Γ , X and L in $\text{AlP}_x\text{Sb}_{1-x}$ are plotted against the alloy concentration x in Figs. 3a and 3b using the VCA alone and the improved VCA, respectively. Our results (Fig. 3a) shows that when the compositional disorder effect is neglected, we predict no transition between the direct and indirect band-gaps and hence the material of interest is expected to remain an indirect (Γ -X) band-gap semiconductor within the whole alloy composition x . Nevertheless, the situation appears to be completely different when the improved VCA is used (Fig. 3b) where we note that the material in question has an indirect (Γ -X) band-gap semiconductor in the alloy composition range 0-0.076, then there is a transition between the indirect band-gaps which occurs twice. First, at composition $x \approx 0.076$ which corresponds to a crossover band gap of 1.169 eV. This transition is originated by L-conduction band. The second transition is found to occur at $x \approx 0.24$ and corresponds to a crossover band gap of 0.886 eV. This transition is predicted to be originated by X-conduction band. Accordingly, the absorption at the optical gaps in $\text{AlP}_x\text{Sb}_{1-x}$ ternary alloys can be either indirect (Γ -X) or indirect (Γ -L) depending on the P content.

The refractive index (n) of semiconducting materials is an important parameter for the design and fabrication of devices. In the present work n has been calculated using various models all of which are based on energy gap-refractive index relations in semiconductors^{25,26}. All energy band-gaps values considered in the calculations are taken with the improved VCA. Our results regarding n for $\text{AlP}_x\text{Sb}_{1-x}$ ($x=0$, $x=0.5$ and $x=1$) are listed in Table 3. The experimental data reported in Ref.²⁷ are also shown for comparison. Note that a combination between the values of n determined for the end-point compounds AlSb and AlP indicates that the Reddy and Anjaneyulu model²⁸ is the most suitable to choose among the remaining models being considered in the present study. This is consistent with the result of Al-Assiri and Bouarissa²⁹. The Reddy and Anjaneyulu²⁸ model is based on the Moss relation²⁵ and expressed as,

$$E_g e^n = 36.3 \quad (5)$$

where E_g is the fundamental energy band-gap. The relation (5) holds true for energy band-gaps larger than 0 eV. Our calculated n for $\text{AlP}_{0.5}\text{Sb}_{0.5}$ is a prediction. The composition dependence of n calculated using the various models of interest is illustrated in Fig.4. Note that for all models being used here, n decreases with increasing x exhibiting a non linear and non-monotonic behavior.

Based on the values of n calculated from the Reddy and Anjaneyulu model²⁸, the high-frequency dielectric constant (ϵ_∞) in $\text{AlP}_x\text{Sb}_{1-x}$ has been determined using the relation

$$\epsilon_\infty = n^2 \quad (6)$$

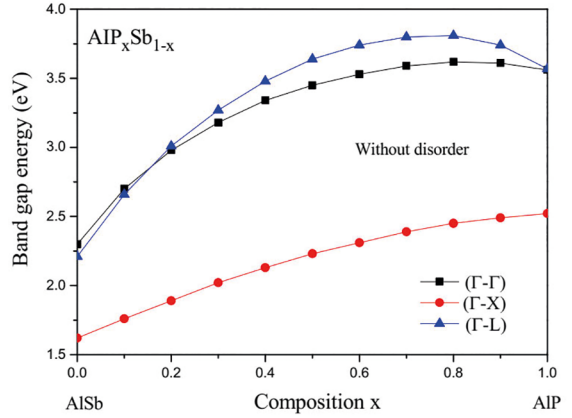


Fig. 3(a)

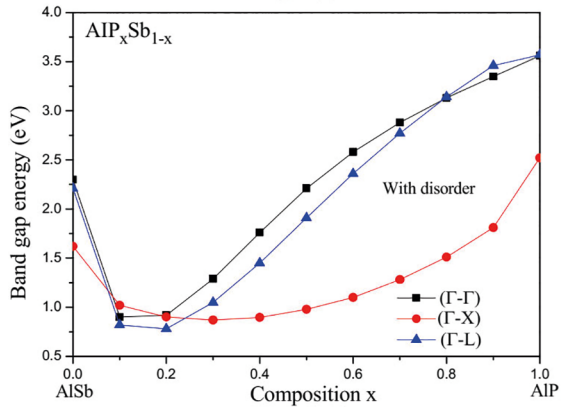


Fig. 3(b)

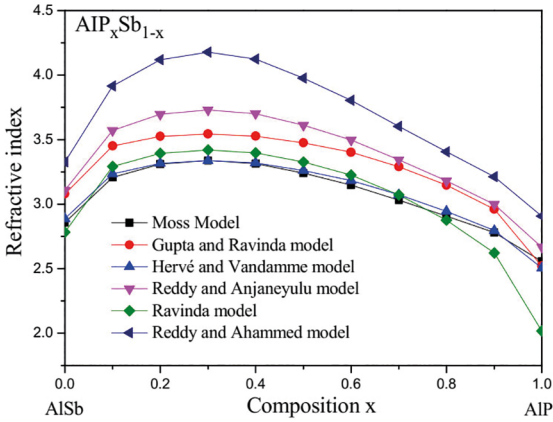
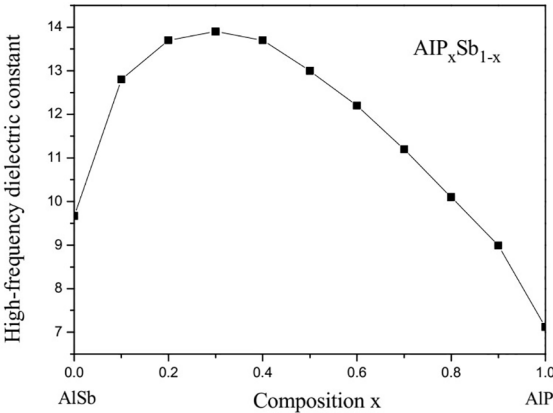
Figure 3. (a). Direct (Γ - Γ) and indirect (Γ -X) and (Γ -L) band gap energies in $\text{AlP}_x\text{Sb}_{1-x}$ ternary alloys versus P content calculated without considering the compositional disorder effect. **(b).** Direct (Γ - Γ) and indirect (Γ -X) and (Γ -L) band gap energies in $\text{AlP}_x\text{Sb}_{1-x}$ ternary alloys versus P content calculated with considering the compositional disorder effect.

The values of ϵ_∞ for AlSb and AlP calculated in the present work are 9.67 and 7.12, respectively. As compared to the experimental values of 9.88 (for AlSb) and 7.4 (for AlP) quoted in Ref.³⁰, an agreement to within 2-4% is achieved. The composition dependence of ϵ_∞ in $\text{AlP}_x\text{Sb}_{1-x}$ ternary system is shown in Fig.5. We observe that the increase of the composition x on going from 0 (AlSb) to 1 (AlP) leads to the non-monotonic decrease of ϵ_∞ . This suggests that $\text{AlP}_x\text{Sb}_{1-x}$ becomes gradually a good insulator when increasing the P content.

The study of electron charge distribution in semiconductors provides important information on the chemical bonding properties and interstitial impurities in the investigated materials³¹⁻³³. For that purpose, the electron total valence charge distribution is calculated at the Γ point along the $[111]$ direction for zinc-blende AlSb, $\text{AlP}_{0.05}\text{Sb}_{0.95}$ and $\text{AlP}_{0.1}\text{Sb}_{0.9}$. Our results are illustrated in Figs. 6a-6c. Note that for zinc-blende

Table 3. Refractive index (n) for AlSb , $\text{AlP}_{0.50}\text{Sb}_{0.50}$ and AlP semiconductor materials calculated using six models.

Material	n calculated from						Expt. [27]
	Moss model	Gupta and Ravindra model	Hervé and Vandamme model	Reddy and Anjaneyulu model	Ravindra model	Reddy and Ahammed model	
AlSb	2.86	3.08	2.89	3.11	2.78	3.33	3.2327
$\text{AlP}_{0.50}\text{Sb}_{0.50}$	3.24	3.48	3.26	3.61	3.33	3.98	-
AlP	2.56	2.52	2.51	2.67	2.02	2.91	2.75

**Figure 4.** Refractive index in $\text{AlP}_x\text{Sb}_{1-x}$ ternary alloys versus P content calculated using various models.**Figure 5.** High-frequency dielectric constant in $\text{AlP}_x\text{Sb}_{1-x}$ ternary alloys versus P content calculated using Reddy and Anjaneyulu model²⁵.

AlSb (Fig. 6a), there is an asymmetrical distribution of charges where an important amount lies between the atomic sites. This seems to be different from that reported for semiconductors with diamond structure³⁴ where the charge distribution is found to be equally distributed between the atomic sites. This reflects the presence of mixed-ionic-covalent bonding in the case of zinc-blende AlSb . The maximum of the electron valence charge density appears to be slightly shifted towards the anion (Sb). Thus, the main contribution to the chemical bond formation comes from the anion. A small amount of charges seems to be in the interstitial regions where it is a

little bit larger in the interstitial region nearest to the cation. When more P atoms are added in AlSb (Figs. 6b and 6c), the shape of the profiles of the electron charge distribution of $\text{AlP}_{0.05}\text{Sb}_{0.95}$ and $\text{AlP}_{0.1}\text{Sb}_{0.9}$ (with disorder) looks like almost the same. Nevertheless, the charge distribution is affected both at anion and cation sites reflecting the change in the ionicity character of the materials of interest. In addition, the maximum of the electron valence charge density decreases by increasing the P content in $\text{AlP}_x\text{Sb}_{1-x}$ affecting thus the contribution to the chemical bond formation. The effect of the compositional disorder on the electron total valence charge density appears to be significant as can be observed in Figs. 6b and 6c. Hence, this effect should be taken in any calculation of the electron valence charge distribution in $\text{AlP}_x\text{Sb}_{1-x}$ ternary alloys.

We have also computed the electron charge densities along the [111] direction for the first conduction band at the Γ -point in the Brillouin zone for zinc-blende AlSb , $\text{AlP}_{0.05}\text{Sb}_{0.95}$ and $\text{AlP}_{0.1}\text{Sb}_{0.9}$. Our results are shown in Figs. 7a-7c, respectively. Note that for AlSb (Fig. 7a), the majority of the charges are localized around the site of the anion (Sb) where it reaches the maximum. Compared to the anion, the amount of charges around the cation (Al) is less pronounced. In the bonding region, we observe the minimum of the electron conduction charge density which is localized almost half way. This indicates that the first conduction band charge density is antibonding and s-like in nature. The trend seems to be similar for III-V semiconductor ternary alloys²⁶. A small quantity of charge can be observed in the interstitial regions but seems to be more important nearest to the cation than the anion. When more P atoms are added in AlSb (Figs. 1b and 1c with disorder), the amount of the charges localized around the anion site decreases whereas those situated around the cation site increases. Thus, it appears that there is a transfer of charges from the anion to the cation site. In the bonding region, the situation seems to be practically constant keeping thus the antibonding and s-like in nature character for the first conduction band charge distribution in the alloys of interest. The effect of compositional disorder in $\text{AlP}_x\text{Sb}_{1-x}$ again is significant for the electron charge density for the first conduction band as clearly seen in Figs. 1b and 1c and can seriously affect the calculation if it is not taken into consideration.

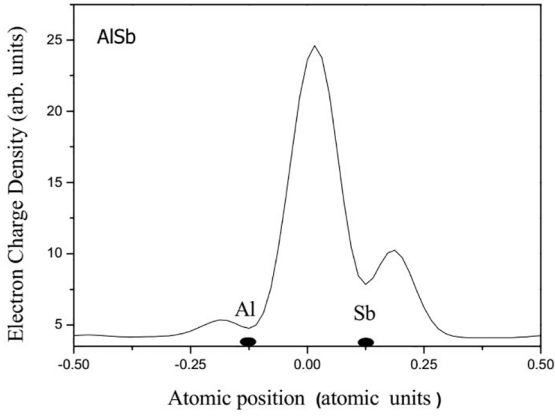


Fig. 6 a

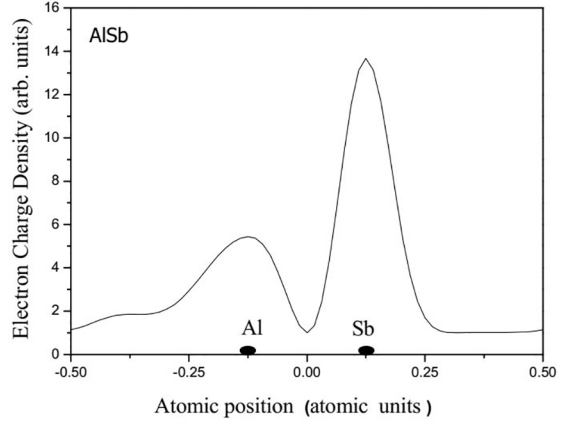


Fig. 7 a

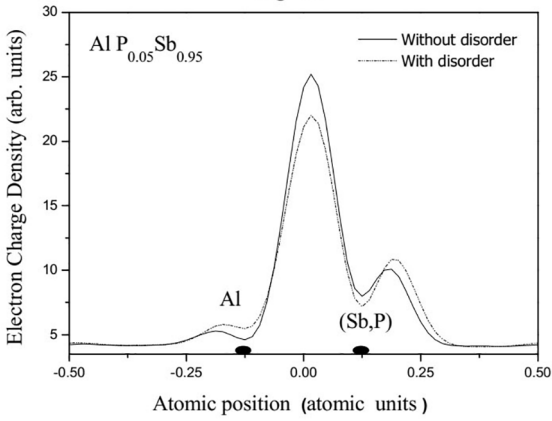


Fig. 6 b

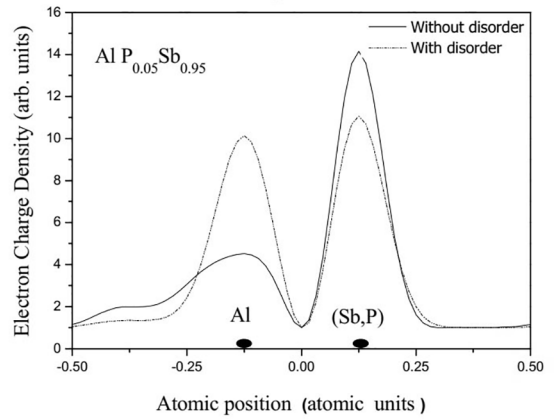


Fig. 7 b

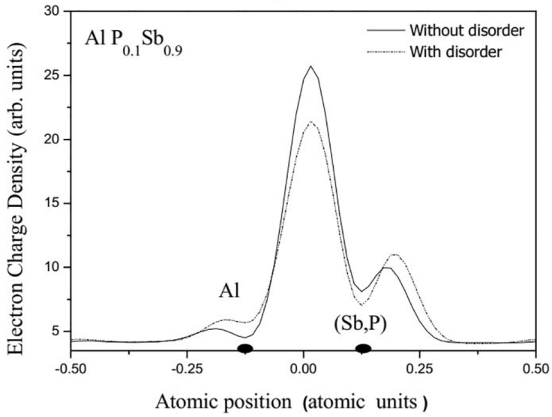


Fig. 6 c

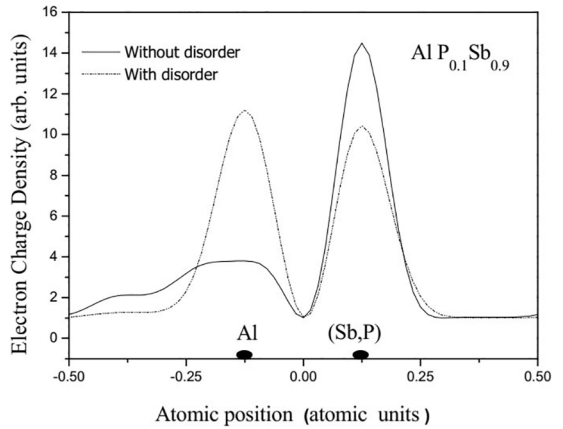


Fig. 7 c

Figure 6. (a) Electron total valence charge density at the Γ point along the [111] direction for AlSb. **(b)** Electron total valence charge density at the Γ point along the [111] direction for $\text{AlP}_{0.05}\text{Sb}_{0.95}$. **(c)** Electron total valence charge density at the Γ point along the [111] direction for $\text{AlP}_{0.1}\text{P}_{0.9}$.

Figure 7. (a) First conduction band charge density at the Γ -point along the [111] direction for AlSb. **(b)** First conduction band charge density at the Γ -point along the [111] direction for $\text{AlP}_{0.05}\text{Sb}_{0.95}$. **(c)** First conduction band charge density at the Γ -point along the [111] direction for $\text{AlP}_{0.1}\text{P}_{0.9}$.

4. Conclusion

Using the EPM within the VCA, the electronic band structure, energy band-gaps at the three major valleys at Γ , X and L, the refractive index and the high-frequency dielectric constant and the electron charge distribution in $\text{AlP}_x\text{Sb}_{1-x}$ ternary semiconductor alloys were calculated. A correction was introduced to the VCA in order to take into account of the compositional disorder effect. Our results were found to be in good accord with experiment. The contribution of the compositional disorder effect to the electron band structure, direct and indirect band-gaps and electron valence and conduction charge densities in $\text{AlP}_x\text{Sb}_{1-x}$ was found to be important and should not be neglected. The composition dependence of all features of interest showed a non-linear behavior. The nature of the semiconductor band-gap was found to depend on the concentration P. In agreement with previous studies, the model of Reddy and Anjaneyulu was chosen among other models being considered in the present study. The behaviour of the high-frequency dielectric constant indicated that $\text{AlP}_x\text{Sb}_{1-x}$ material becomes a good insulator when more P atoms are incorporated. The behaviour of the charge distribution showed an ionic partial character for the alloys of interest.

5. References

- Vurgaftman I, Meyer JR, Ram-Mohan LR. Band parameters for III-V compound semiconductors and their alloys. *Journal of Applied Physics*. 2001;89(11):5815.
- Bouarissa N. Band gaps and charge distribution in quasi-binary $(\text{GaSb})_{1-x}(\text{InAs})_x$ crystals. *European Physical Journal B*. 2003;32(2):139-143.
- Bouarissa N. Phonons and related crystal properties in indium phosphide under pressure. *Physica B: Condensed Matter*. 2011;406(13):2583-2587.
- Othman M, Kasap E, Korozlu N. The structural, electronic and optical properties of $\text{In}_x\text{Ga}_{1-x}\text{P}$ alloys. *Physica B: Condensed Matter*. 2010;405(10):2357-2361.
- Sürücü G, Colakoglu K, Deligoz E, Ciftci Y, Korozlu N. Electronic, elastic and optical properties on the $\text{Zn}_{1-x}\text{Mg}_x\text{Se}$ mixed alloys. *Journal of Materials Science*. 2011;46(4):1007-1014.
- Hannachi L, Bouarissa N. Electronic structure and optical properties of $\text{CdSe}_x\text{Te}_{1-x}$ mixed crystals. *Superlattices and Microstructures*. 2008;44(6):794-801.
- Meyer JR, Olafsen LJ, Aifer EH, Bewley WW, Felix CL, Vurgaftman I, et al. Type II W, interband cascade and vertical-cavity surface-emitting mid-IR lasers. *IEE Proceedings - Optoelectronics*. 1998;145(5):275-280.
- Chow DH, Dunlap HL, Williamson W, Enquist S, Gilbert BK, Subramaniam S, et al. InAs/AlSb/GaSb resonant interband tunneling diodes and Au-on-InAs/AlSb-superlattice Schottky diodes for logic circuit. *IEEE Electron Device Letters*. 1996;17(2):69-71.
- Shimomura H, Anan T, Sugou S. Growth of AlPSb and GaPSb on InP by gas-source molecular beam epitaxy. *Journal of Crystal Growth*. 1996;162(3-4):121-125.
- Glisson TH, Hauser JR, Littlejohn MA, Williams CK. Energy bandgap and lattice constant contours of iii-v quaternary alloys. *Journal of Electronic Materials*. 1978;7(1):1-16.
- Cohen ML, Chelikowsky JR. *Electronic Structure and Optical Properties of Semiconductors*. Berlin: Springer-Verlag; 1988.
- Harrison P. *Quantum Wells, Wires and Dots: Theoretical and Computational Physics of Semiconductor Nanostructures*. Chichester: Wiley; 2000.
- Bouarissa N, Bougouffa S, Kamli A. Energy gaps and optical phonon frequencies in $\text{InP}_{1-x}\text{Sb}_x$. *Semiconductor Science and Technology*. 2005;20(3):265.
- Bouarissa N. Electronic properties of $\text{Ga}_x\text{In}_{1-x}\text{P}$ from pseudopotential calculations. *Materials Chemistry and Physics*. 2010;124(1):336-341.
- Kobayasi T, Nara H. Properties of nonlocal pseudopotentials of Si and Ge optimized under full interdependence among potential parameters. *Bulletin of College of Medical Sciences, Tohoku University*. 1993;2(1):7-16.
- Bechiri A, Bouarissa N. Energy band gaps for the $\text{Ga}_x\text{In}_{1-x}\text{As}_y\text{P}_{1-y}$ alloys lattice matched to different substrates. *Superlattices and Microstructures*. 2006;39(6):478-488.
- Bouarissa N, Boucenna M. Band parameters for AlAs, InAs and their ternary mixed crystals. *Physica Scripta*. 2009;79(1):015701.
- Alibert C, Joullié A, Joullié AM, Ance C. Modulation-spectroscopy study of the $\text{Ga}_{1-x}\text{Al}_x\text{Sb}$ band structure. *Physical Review B*. 1983;27(8):4946.
- Lee SJ, Kwon TS, Nahm K, Kim CK. Band structure of ternary compound semiconductors beyond the virtual crystal approximation. *Journal of Physics: Condensed Matter*. 1990;2(14):3253-3258.
- Bouarissa N. Effects of compositional disorder upon electronic and lattice properties of $\text{Ga}_x\text{In}_{1-x}\text{As}$. *Physics Letters A*. 1998;245(3-4):285-291.
- Bouarissa N. Pseudopotential calculations of $\text{Cd}_{1-x}\text{Zn}_x\text{Te}$: Energy gaps and dielectric constants. *Physica B: Condensed Matter*. 2007;399(2):126-131.
- Vegard L. Die Konstitution der Mischkristalle und die Raumfüllung der Atome. *Zeitschrift für Physik*. 1921;5(1):17-26.
- Bechiri A, Benmakhlof F, Bouarissa N. Band structure of III-V ternary semiconductor alloys beyond the VCA. *Materials Chemistry and Physics*. 2003;77(2):507-510.
- Kassali K, Bouarissa N. Composition and temperature dependence of electron band structure in $\text{ZnSe}_{1-x}\text{S}_x$. *Materials Chemistry and Physics*. 2002;76(3):255-261.

25. Ravindra NM, Ganapathy P, Choi J. Energy gap-refractive index relations in semiconductors - An overview. *Infrared Physics & Technology*. 2007;50(1):21-29.
26. Fares NEH, Bouarissa N. Energy gaps, charge distribution and optical properties of $\text{Al}_x\text{In}_{1-x}\text{Sb}$ ternary alloys. *Infrared Physics & Technology*. 2015;71:396-401.
27. Weber MJ, ed. *Handbook of Optical Materials*. Berlin: Springer; 2003.
28. Reddy RR, Anjaneyulu S. Analysis of the Moss and Ravindra relations. *Physica Status Solid (b)*. 1992;174(2):k91-k93.
29. Al-Assiri MS, Bouarissa N. Electronic band structure and derived properties of $\text{AlAs}_x\text{Sb}_{1-x}$ alloys. *Superlattices and Microstructures*. 2013;59:144-154.
30. Adachi S. *Properties of Group - IV, III-V, and II-VI Semiconductors*. Chichester: Wiley; 2005.
31. Richardson SL, Cohen ML, Louie SG, Chelikowsky JR. Electron charge densities at conduction-band edges of semiconductors. *Physical Review B: Condensed Matter*. 1986;33(2):1177-1182.
32. Bouarissa N. Electron valence charge densities in $\text{Hg}_{1-x}\text{Cd}_x\text{Te}$ mixed crystals. *Infrared Physics & Technology*. 1998;39(5):265-270.
33. Bouarissa N. Electronic structure and lattice properties of zincblende InN under high pressure. *European Physical Journal B*. 2002;26(2):153-158.
34. Bouarissa N, Annane F. Electronic properties and elastic constants of the ordered $\text{Ge}_{1-x}\text{Sn}_x$ alloys. *Materials Science and Engineering: B*. 2002;95(2):100-106.